Video Article

Induction and Diagnosis of Tumors in *Drosophila* Imaginal Disc Epithelia

Kenta Morimoto[1,2], Yoichiro Tamori[1]

[1]Structural Biology Center, National Institute of Genetics and Department of Genetics, School of Life Science, SOKENDAI

[2]Graduate School of Media and Governance, Keio University

Correspondence to: Yoichiro Tamori at yotamori@nig.ac.jp

URL: https://www.jove.com/video/55901
DOI: doi:10.3791/55901

Keywords: Cancer Biology, Issue 125, Drosophila, Imaginal disc, Tumorigenesis, Neoplasia, Dysplasia, Tumor suppressor gene, GAL4-UAS, RNAi

Date Published: 7/25/2017

Citation: Morimoto, K., Tamori, Y. Induction and Diagnosis of Tumors in *Drosophila* Imaginal Disc Epithelia. *J. Vis. Exp.* (125), e55901, doi:10.3791/55901 (2017).

Abstract

In the early stages of cancer, transformed mutant cells show cytological abnormalities, begin uncontrolled overgrowth, and progressively disrupt tissue organization. *Drosophila melanogaster* has emerged as a popular experimental model system in cancer biology to study the genetic and cellular mechanisms of tumorigenesis. In particular, genetic tools for *Drosophila* imaginal discs (developing epithelia in larvae) enable the creation of transformed pro-tumor cells within a normal epithelial tissue, a situation similar to the initial stages of human cancer. A recent study of tumorigenesis in *Drosophila* wing imaginal discs, however, showed that tumor initiation depends on the tissue-intrinsic cytoarchitecture and the local microenvironment, suggesting that it is important to consider the region-specific susceptibility to tumorigenic stimuli in evaluating tumor phenotypes in imaginal discs. To facilitate phenotypic analysis of tumor progression in imaginal discs, here we describe a protocol for genetic experiments using the GAL4-UAS system to induce neoplastic tumors in wing imaginal discs. We further introduce a diagnosis method to classify the phenotypes of clonal lesions induced in imaginal epithelia, as a clear classification method to discriminate various stages of tumor progression (such as hyperplasia, dysplasia, or neoplasia) had not been described before. These methods might be broadly applicable to the clonal analysis of tumor phenotypes in various organs in *Drosophila*.

Video Link

The video component of this article can be found at https://www.jove.com/video/55901/

Introduction

Epithelial tissues are highly organized systems that have the remarkable homeostatic ability to maintain their organization through development and cell turnover. This robust self-organizing system, however, is progressively disrupted during tumor development. At the beginning of tumor development, individual mutant cells arising from oncogene activation or tumor-suppressor gene inactivation emerge within an epithelial layer. When this transformed "pro-tumor cell" evades a suppressive environment, disrupts epithelial organization, and begins uncontrolled proliferation, tumorigenesis occurs [1]. During the past few decades, outstanding technological advances in genetics and molecular biology have made remarkable progresses on cancer research. In particular, recent studies using the genetically mosaic analysis tools in *Drosophila melanogaster*, such as FLP-FRT (flippase recombinase/flippase recombinase target) mitotic recombination [2] and flip-out-GAL4-UAS (upstream activating sequence) systems [3], have greatly contributed to better understanding the genetic mechanisms involved in the formation and metastasis of tumors [4,5,6].

Studies of a group of conserved *Drosophila* tumor-suppressor genes, *lethal giant larvae* (*lgl*), *discs large* (*dlg*), and *scribble* (*scrib*), highlighted the critical relationship between loss of epithelial organization and tumor development, as these genes play key roles in regulation of apical-basal cell polarity and cell proliferation in epithelial tissues [7]. While *Drosophila* imaginal discs are normally monolayered epithelia, homozygous mutations in any of these three genes cause cells to lose structure and polarity, fail to differentiate, overproliferate, and ultimately form multilayered amorphous masses that fuse with adjacent tissues [7]. Similarly, disruption of these genes in mammals is involved in the development of malignant tumors [8,9]. The neoplastic phenotypes exhibited by the mutant tissues have led to the classification of these three genes as conserved, neoplastic tumor-suppressor genes (nTSGs) [7,8]. However, when homozygous nTSG mutant cells are sporadically generated in developing wild-type imaginal discs using FLP-FRT-mediated mitotic recombination, mutant cells are eliminated from the tissue through c-Jun N-terminal kinase (JNK)-dependent apoptosis [10,11,12,13,14], extrusion [15,16], or engulfment and phagocytosis by neighbors [17]. In this genetically mosaic epithelia, apoptosis is mostly detected in nTSG mutant cells located at the clone boundary, suggesting that adjacent normal cells trigger the apoptosis of nTSG mutant cells [10,11,12,18]. Recent studies in mammalian cells have confirmed that this cell competition-dependent elimination of pro-tumor cells is an evolutionarily conserved epithelial self-defense mechanism against cancer [19,20,21,22,23].

A recent study in *Drosophila* imaginal discs, however, showed that mosaic nTSG-knockdown clones induces neoplastic tumors in specific regions of wing imaginal discs [16]. Initial tumor formation was always found in the peripheral "hinge" region and never observed in the central "pouch" region of the wing disc epithelium, suggesting that the tumorigenic potential of nTSG-knockdown cells depends on the local environment. The central pouch region functions as a "tumor coldspot" where pro-tumor cells do not show dysplastic overgrowth, whereas the peripheral hinge region behaves as a "tumor hotspot" [16]. In "coldspot" pouch regions, nTSG-knockdown cells delaminate from the basal side and undergo apoptosis. In contrast, as "hotspot" hinge cells possess a network of robust cytoskeletal structures on their basal sides,

Copyright © 2017 Journal of Visualized Experiments

nTSG-knockdown cells delaminate from the apical side of the epithelium and initiate tumorigenic overgrowth [16]. Therefore, analysis of tumor phenotypes in imaginal discs requires careful consideration of the region-specific susceptibility to tumorigenic stimuli.

Here, we describe a protocol to induce neoplastic tumor formation in the *Drosophila* wing imaginal discs utilizing the GAL4-UAS-*RNAi* system by which nTSG-knockdown cells are generated in normal wing disc epithelia. Although these experimental systems are useful to study the early stages of cancer, a clear classification method to evaluate the stages of tumor progression in imaginal disc epithelia has not been clearly described before. Therefore, we also propose a diagnosis method to classify pro-tumor clonal phenotypes induced in the wing disc epithelia into three categories: hyperplasia (accumulation of an excessive number of normal-appearing cells with increased proliferation), dysplasia (premalignant tissue composed of abnormally appearing cells), and neoplasia (benign or malignant tumor composed of cells having an abnormal appearance and abnormal proliferation pattern).

Protocol

1. Fly Crosses and Clone Induction

1. Remove all flies in the vial 12 h before collecting virgin flies.
2. Anesthetize the flies in the vial by injecting CO_2 gas and place flies onto a CO_2 fly pad.
3. Transfer 10 - 20 virgin females and 10 males from the CO_2 fly pad into a fresh vial and incubate for 1 day at 25 °C.
4. Transfer these flies into a fresh vial and incubate for 12 h at 25 °C.
   NOTE: Discard the first vial as virgin females do not lay enough eggs in the first day.
5. For enhancer-GAL4 lines, remove the adult flies and incubate the vial at 25 °C until dissection.
6. For induction of mosaic clones by flip-out-GAL4, remove the adult flies and incubate the vial for 2 - 4 days at 25 °C. The incubation time before heat shock is dependent on the experimental purpose. A heat shock 2 days after egg deposition (AED) generates mosaic clones in immature second instar imaginal epithelia. A heat shock after 3 or 4 days AED generates mosaic clones in differentiated early- to mid-third instar imaginal epithelia.
   NOTE: It is important to examine the effect of altered heat-shock timing on tumorigenic phenotypes.
7. For induction of mosaic clones by flip-out-GAL4, heat shock the vial by immersion in a 37 °C water bath for 10 - 45 min followed by incubation for 2 - 3 days at 25 °C.
   NOTE: Information of heat-shock time, timing, and incubation time in each experiment is shown in the figure legends.

2. Dissection of Larvae

1. Collect wandering third instar larvae with a wooden stick or blunt forceps, genotype them by appropriate fluorescent markers (*e.g.*, EGFP) under a fluorescence stereoscopic microscope and place them in a dissection dish with PBS (phosphate buffered saline).
2. Wash the larvae in PBS by pipetting with 2 mL plastic transfer pipettes.
3. Pinch the center of the larva with one forceps and tear the body in half with the other forceps.
4. Pinch the mouth hook of the anterior half with one forceps and push the mouth towards the body with the other forceps to turn the body inside out.
5. Remove unnecessary materials such as salivary glands or fat bodies with forceps.

3. Fixation and Antibody Staining

1. Transfer the dissected anterior half of the larval body (including imaginal wing discs) to a 1.5 mL plastic tube and fix in 1 mL of Fix solution (4% Formaldehyde in PBS) for 10 min at room temperature in the dark with gentle rotation.
   CAUTION: Formaldehyde is toxic and has carcinogenic potential. Wear protective gloves and clothing to prevent skin contact.
   NOTE: In this part, all steps take place on a nutator at room temperature in the dark unless otherwise noted.
2. Remove the Fix solution and discard. Wash the tissues with 1 mL of PBT (0.3% Triton X-100 in PBS) three times for 15 min each.
3. Remove the PBT and add 1 mL of PBTG (0.2% bovine serum albumin and 5% normal goat serum in PBT) for blocking and nutate 1 h at room temperature or overnight at 4 °C.
4. Remove PBTG and add primary antibody solution appropriately diluted with PBTG (see **Materials Table**) and nutate overnight at 4 °C.
5. Remove the primary antibody solution and wash the tissues with 1 mL PBT three times for 15 min each.
6. Remove PBT and add secondary antibody solution appropriately diluted with PBTG (1:400). Nutate for 2 h at room temperature or overnight at 4 °C.
7. Remove secondary antibody solution and wash the tissues with 1 mL of PBT two times for 15 min each.
8. To stain F-actin, remove PBT and add Phalloidin solution appropriately diluted in PBS (1:40). Then nutate for 20 min. Remove the Phalloidin solution and wash the tissues with 1 mL of PBT two times for 15 min each.
9. To counterstain nuclear DNA, remove PBT and add DAPI (4', 6-diamidino-2-phenylindole) solution (0.5 µg/mL of DAPI in PBS). Then nutate 10 min.
   CAUTION: DAPI has carcinogenic potential. Wear protective gloves and clothing to prevent skin contact.
10. Remove DAPI solution and wash the tissues with 1 mL of PBT two times for 15 min each.
11. Rinse once in 1 mL of PBS for 10 min at room temperature.
12. Remove PBS and add 500 µL of 100 % glycerol as the pre-mounting medium.

4. Mounting onto Microscope Slides

1. Place the stained tissues on a microscope slide using a 2 mL plastic transfer pipette.

2. Transfer the tissues to drops of mounting medium on another microscope slide with forceps.
3. Hold down the end of dissected tissue with one forceps and pull away brain and eye antennal discs with the other forceps.
   NOTE: Keep the dissected brains to place them near the wing imaginal discs. The brains act as a platform preventing the coverslip from crushing the wing imaginal discs.
4. To isolate the wing imaginal discs hold down the end of dissected tissue with one forceps and gently scratch the body wall and tear off the discs with the other forceps.
   NOTE: If it is difficult to find wing imaginal discs, peel the trachea from the posterior to the anterior side. Wing imaginal discs stick to the trachea.
5. Gently cover the imaginal discs with a coverslip and seal with nail polish; store at 4 °C.

5. Confocal Microscopy

1. To acquire confocal images using a confocal microscope set image acquisition parameters including range of emission wavelength, laser intensity, gain, offset, scanning speed and image size [24].
   NOTE: For detailed procedure of image acquisition settings, refer to the instruction manual supplied by each microscope manufacturer.
2. To capture single confocal sections of an entire wing imaginal disc, use a 20X objective lens.
3. Acquire 3-dimensional images by z-stack scanning at step-size of 0.5 - 1.0 µm using 40X or 60X lenses.
   NOTE: To analyze cellular phenotypes in high resolution, an image size should be larger than 512 x 512 pixels.

6. Image Analysis Using ImageJ

1. Use Fiji, an open-source ImageJ software focused on biological-image analysis (https://fiji.sc/) [25], to acquire and analyze confocal z-stack images.
2. To acquire vertical sections, open the z-stack images in ImageJ and select the menu item "Image/Stacks/Reslice."
   NOTE: Either X-Z axis or Y-Z axis are selectable in the Reslice menu. Vertical section can be obtained also in an arbitrary direction by drawing a straight line or rectangle onto the z-stack image.

7. Diagnosis of Neoplastic Phenotypes

1. Open the vertical sections (X-Z or Y-Z axis) obtained from one set of z-stack images and analyze morphological phenotypes and antibody staining.
2. For the diagnosis of tumor phenotypes, mainly focus on the following three points: (1) if a cell mass, including knockdown clones, deviates from the main epithelial layer, (2) if the subcellular localization of junctional proteins is altered in this cell mass, and (3) if the diameter of this cell mass is larger than 4 cells.
3. Categorize tumor phenotypes according to the flowchart described in **Figure 1**.

Representative Results

To demonstrate neoplastic tumor formation experimentally induced by *RNAi*-mediated nTSG-knockdown in *Drosophila* wing imaginal discs, three different GAL4 drivers were used to express *UAS-RNAi* for *lgl* or *scrib*: (1) *sd-GAL4,* which drives strong UAS expression in the wing pouch and mild expression in the hinge regions (**Figure 2** and **Figure 3A**); (2) *upd-GAL4,* which drives in subdomains of the hinge, including strong expression in two domains of the dorsal medial fold, mild expression in one anterior-lateral domain, and weak expression in the ventral-posterior domain (**Figure 2** and **Figure 3C**); and (3) heat-shock-induced flip-out GAL4, which generates random mosaic clones expressing UAS-genes (**Figure 4** and **Figure 5**). In all of the experiments, *UAS-EGFP* was co-expressed with *UAS-RNAi* to mark the knockdown clones.

First, *sd-GAL4*-driven *lgl-RNAi* was used to induce knockdown of *lgl* in the wing pouch and hinge regions. In control third instar wing discs without *UAS-lgl-RNAi*, no morphological alteration occurred (**Figure 3A**). In contrast, in third instar wing discs expressing *lgl-RNAi*, epithelial deformations and tumorigenic overgrowths were clearly observed in certain parts of the hinge (**Figure 3B**). In the wing pouch region, however, dysplastic overgrowth was not observed. Strong MMP1 (matrix metalloprotease-1) expression was observed in the tumorous hinge lesions but not in the wing pouch region (**Figure 3B**). Since MMP1 expression is involved in degradation of basement membranes, it is possible that these hinge tumors have a metastatic capability (**Figure 3B**). Next, *upd-GAL4* was used to induce *lgl* knockdown in the hinge region. In control third instar wing discs without *UAS-lgl-RNAi*, no morphological alterations occurred (**Figure 3C**). However, after 5 days AED, third instar wing discs with *upd-GAL4* and *lgl-RNAi* displayed prominent epithelial disorganization, with F-actin accumulation and clone displacement from the epithelial layer (**Figure 3D**). At 6 days AED, neoplastic tumors expressing MMP1 overgrew in the hinge region (**Figure 3G**), albeit with variation in tumor size between samples (**Figure 3E and F**). A vertical section of the hinge region confirmed that the neoplastic tumor underwent deviating outgrowth at the apical side of epithelial layer (**Figure 3H**).

To monitor the progression of tumor growth induced by *lgl* knockdown, sporadic clones expressing *lgl-RNAi* were generated in wing discs using the heat-shock-induced flip-out GAL4 mosaic system. Two days after heat-shock to second instar larvae (2 days AED), some *lgl*-knockdown clones located in the hinge region showed deviation away from the apical side of the epithelial layer (**Figure 4A**). Four days after heat-shock induction, dysplastic lesions in the hinge region became clear, suggesting that *lgl*-knockdown clones displaced away from the apical side proliferate in the lumen (**Figure 4B**). Seven days after heat-shock induction, tumorigenic overgrowths dominated the hinge regions (**Figure 4C**).

To demonstrate the classification of clonal phenotypes with our diagnosis method, sporadic clones expressing *scrib-RNAi* were generated in wing discs using the heat-shock-induced flip-out GAL4 mosaic system. Five days after heat-shock to second instar larvae (2 days AED), certain GFP-expressing *scrib*-knockdown clones showed tumorigenic phenotypes (**Figure 5A**). We analyzed four clones (B, C, D and E in **Figure 5A**) in vertical sections of z-stack confocal images utilizing ImageJ, because it is difficult to acquire the detailed cytological and structural phenotypes in the 2D confocal images (**Figure 4** and **Figure 5A**). Clones B and C were classified as dysplasia as septate-junction protein Discs large (Dlg)

was mislocalized (**Figure 5B and C**). In clone B, the size of the cell mass displaced from the epithelium was not greater than 4-cells in diameter (**Figure 5B**), while clone C did not deviate from the epithelium (**Figure 5C**); therefore, clones B and C were not considered neoplastic. However, clones D and E, which also showed mislocalization of Dlg, formed tumorous cell masses outside of the epithelium (**Figure 5D** and **5E**). As the size of these displaced tumorous clones was more than 4-cells in diameter, the clones were classified as neoplastic.

To induce hyperplastic tumors or cyst formations in the wing imaginal discs, sporadic clones expressing oncogeneic Ras (Ras^{V12}) or constitutively active form of Yorkie, a transcriptional coactivator of the Hippo pathway, (Yki^{3SA}) were generated using the heat-shock-induced flip-out GAL4 mosaic system. Four days after heat shock to second instar larvae (2 days AED), Ras^{V12}-expressing clones labeled by GFP became round cell masses in the imaginal discs (**Figure 6A**). A vertical section of the Ras^{V12}-expressing clone (clone B in **Figure 6A**) revealed that the cell mass dissociated from the epithelial layer has proper localization of Dlg, suggesting that the cell mass maintains normal epithelial structures outside the epithelial layer (**Figure 6B**). MMP1 expression was not observed in these Ras^{V12}-expressing clones (**Figure 6C**). Therefore, the clone B was classified as cyst formation. Four days after heat shock to second instar larvae (2 days AED), Yki^{3SA}-expressing clones labeled by GFP formed big cell masses in the imaginal discs (**Figure 7A**). We focused on two clones (B and C in **Figure 7A**). Clone B showed integration in the epithelial layer and proper localization of Dlg in the sub-apical membranes of the epithelial cells, suggesting that the Yki^{3SA}-expressing clone B maintained epithelial structure. Therefore, clone B was classified as hyperplasia (**Figure 7B**). Clone C located in the hinge region showed mislocalization of Dlg and formed multi-layered structure at the basal side of the epithelial layer. MMP1 expression was not observed in the Yki^{3SA}-expressing clones. Taken together, clone C was classified as benign neoplasm (**Figure 7C** and **D**).

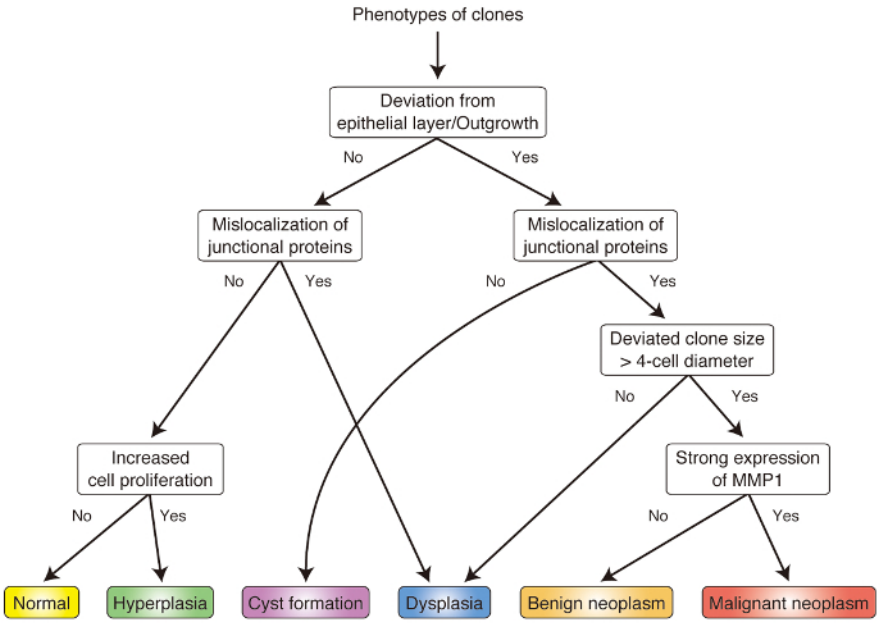

Figure 1: Flowchart for Classification of Tumor Phenotypes. This flowchart represents a diagnosis method to classify clonal lesions in imaginal epithelia. The classification is based on five criteria: (1) deviation of clones from the epithelial layer, (2) subcellular mislocalization of junctional proteins, (3) cellular proliferation, (4) clone size and (5) MMP1 expression. Please click here to view a larger version of this figure.

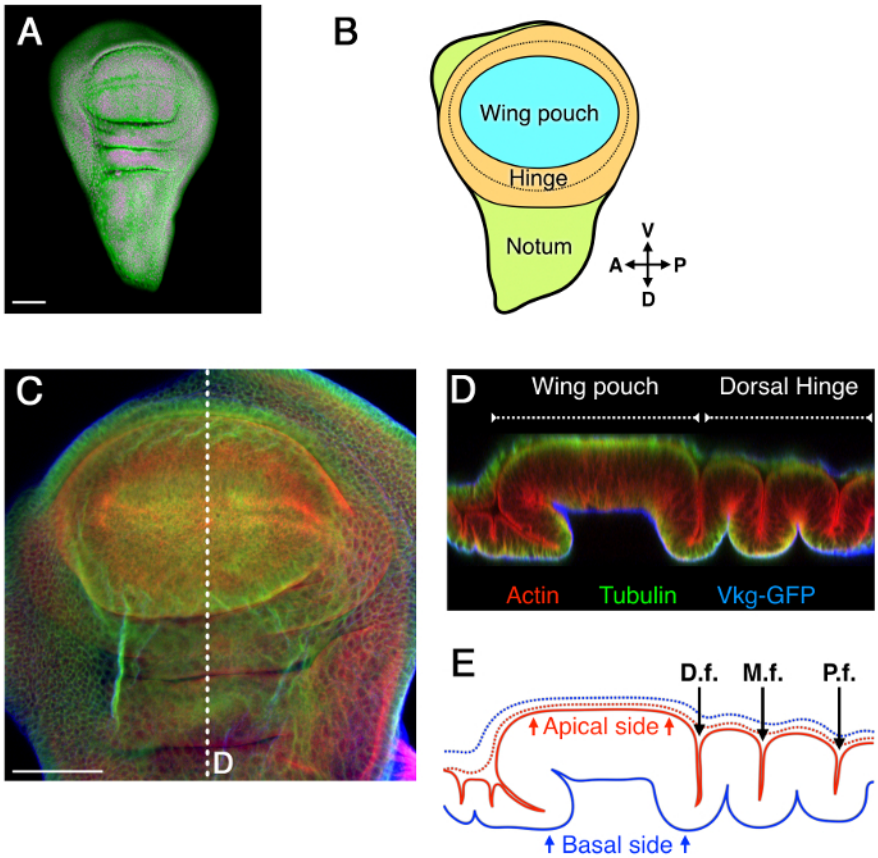

Figure 2: (**A**) Wild-type wing imaginal disc stained for Dlg (green) and nuclei (DAPI, magenta). (**B**) Schematic representation of Drosophila wing imaginal discs showing wing pouch (blue), hinge (orange) and notum (green) regions. (**C**) Normal wing imaginal disc stained for F-actin (red) and microtubules (green). Basement membranes are labeled with Collagen IV/Vkg-GFP (blue). (**D**) Vertical section of the site marked with white dotted line in (**C**). (**E**) Line drawings trace the apical (red) and basal (blue) sides of the epithelial layer in (**D**). Dotted lines trace the peripodial membrane. Distal (D.f.), medial (M.f.) and proximal (P.f.) folds of the dorsal hinge are indicated.
Detailed genotypes: **A,** w^- **C-D,** *Vkg-GFP* Please click here to view a larger version of this figure.

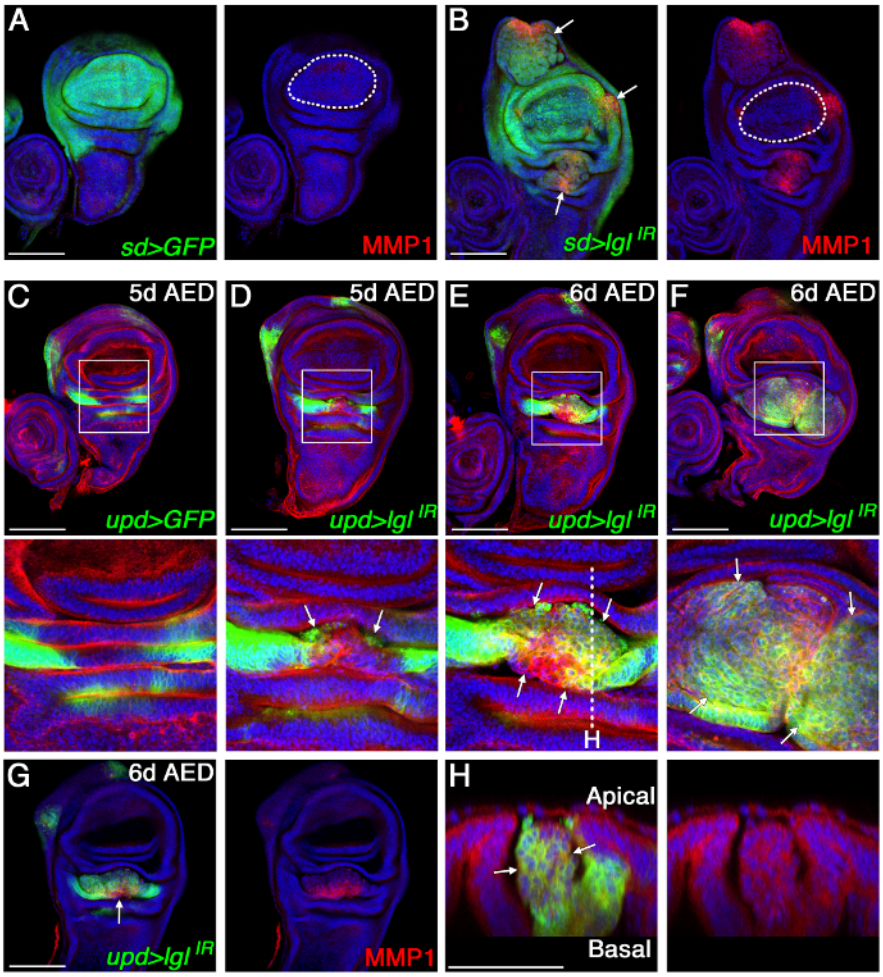

Figure 3: Site-specific Tumorigenesis Induced by Enhancer-GAL4s. (**A**, **B**) Confocal images show wing imaginal discs dissected from third instar larvae of indicated genotypes stained for MMP1 (red). The *sd-GAL4*-expressing regions were labeled by GFP expression (green). (**C-G**) Confocal images show wing imaginal discs dissected from third instar larvae of indicated genotypes at the indicated time point AED. F-actin was stained with Phalloidin (red) in (**C-F**). MMP1 expression is stained with anti-MMP1 antibodies (red) in (**G**). The *upd-GAL4*-expressing regions were labeled by GFP expression (green). Bottom panels of (**C-F**) show magnified views of regions indicated in upper panels. White arrows indicate dysplastic lesions induced by *lgl*-knockdown clones. (**H**) Vertical section of the site marked with white dotted line in the bottom panel of (E). White dotted lines mark the boundaries between wing pouch and hinge regions in (A) and (B). Nuclei were labeled with DAPI (blue). Scale bars = 100 µm in (A-G) and 50 µm in (H). Detailed genotypes: **A,** *w*$^{-}$*, sd-GAL4, UAS-EGFP; UAS-dicer2;* ***B,*** *w*$^{-}$*, sd-GAL4, UAS-EGFP; UAS-dicer2; UAS-lgl-RNAi;* **C,** *w*$^{-}$*, upd-GAL4, UAS-EGFP; UAS-dicer2;* **D-H,** *w*$^{-}$*, upd-GAL4, UAS-EGFP; UAS-dicer2; UAS-lgl-RNAi* Please click here to view a larger version of this figure.

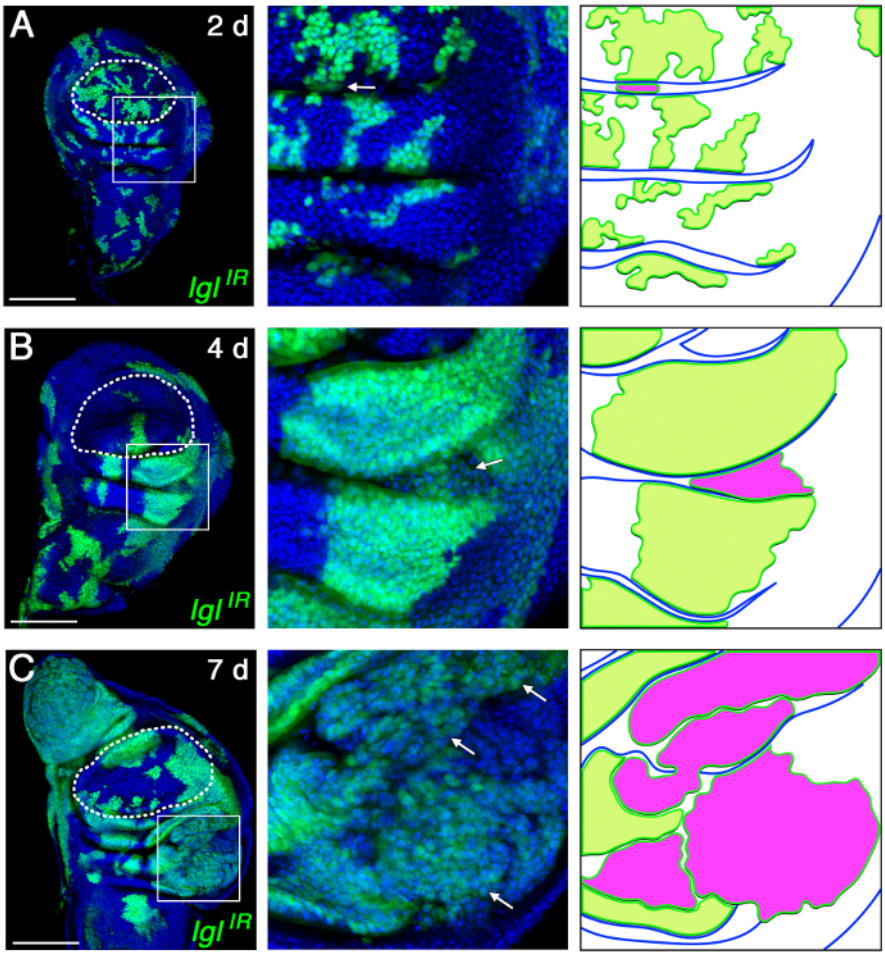

Figure 4: Tumor Phenotypes Induced by Random Mosaic Clones. (**A-C**) Confocal images show mosaic wing imaginal discs of third instar larvae with clones co-expressing *lgl-RNAi* and GFP (green) at the indicated time point after heat-shock induction. Nuclei were labeled by DAPI (blue). The middle panels show magnified views of the white square regions marked in left panels. The right panels show schematic line drawings of the apical side of the epithelial layers (blue) and the GFP-expressing clones (green). Mosaic clones located within the epithelium are depicted in light green while neoplastic tumors deviating from the epithelium are shown in magenta. White dotted lines in the left panels mark the boundaries between wing pouch and hinge regions. White arrows in the middle panels indicate dysplastic lesions induced by *lgl*-knockdown clones. Scale bars = 100 µm. Detailed genotypes: **A-C,** *hsFLP; UAS-dicer2; act>CD2>GAL4, UAS-EGFP/UAS-lgl-RNAi* (heat-shocked 30 min at 2 days AED, incubate 2 days at 25 °C in A, incubate 4 days at 25 °C in B, incubate 7 days at 25 °C in C after heat shock). Please click here to view a larger version of this figure.

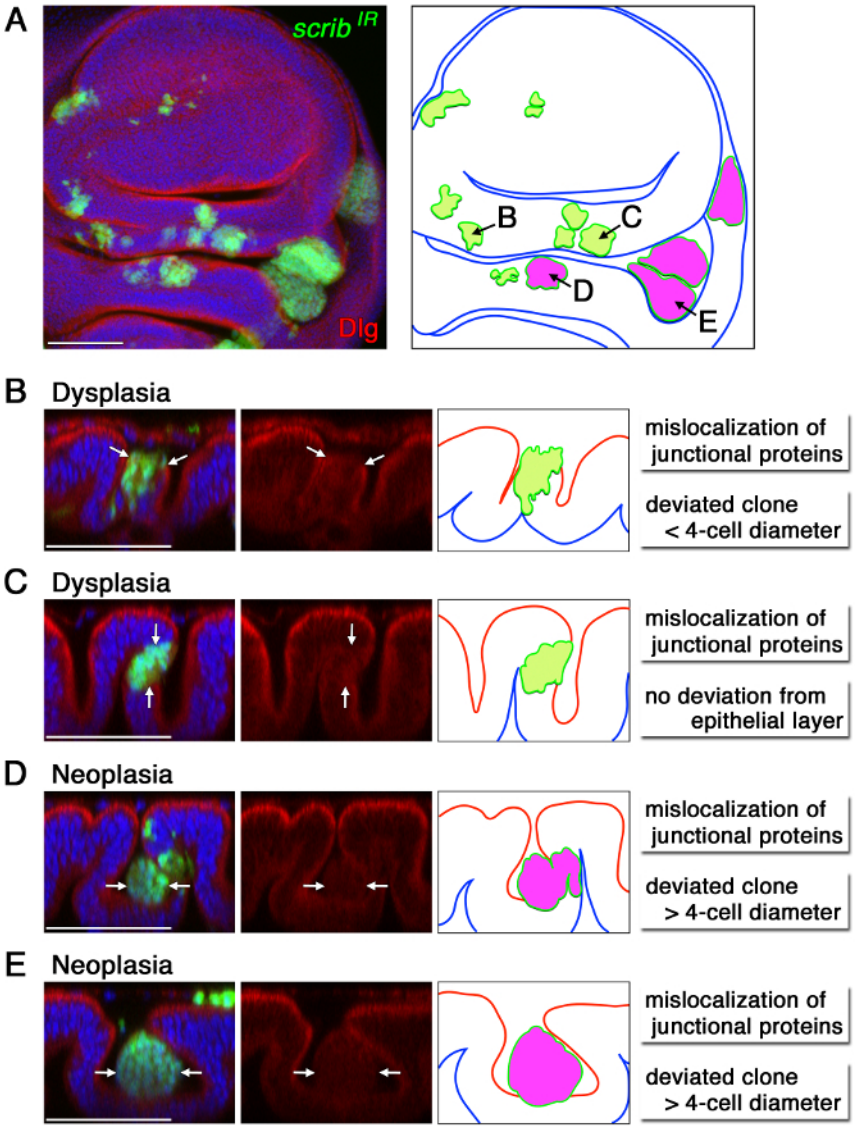

Figure 5: Diagnostic Examination of Dysplastic Clonal Phenotypes. (**A**) The left panel shows a mosaic wing imaginal disc of third instar larva with clones co-expressing *scrib-RNAi* and GFP (green) 5 days after heat-shock induction, stained for Dlg (red). The right panel shows a schematic line drawing of the apical side of the epithelial layers (blue) and the GFP-expressing clones (green). Mosaic clones in the epithelial layers are shown in light green while neoplastic tumors displaced from the epithelium are shown in magenta. (**B-E**) The confocal images show vertical sections of the *scrib*-knockdown clones indicated in the right panel of (A). The second panels from the left show the Dlg localization patterns (red). The third panels from the left show schematic line drawings of the apical (red) and basal (blue) sides of epithelial layers and the GFP-expressing *scrib*-knockdown clones (green). Dysplastic clones in the epithelial layers are shown in light green (B and C) while neoplastic clones displaced from the epithelium are shown in magenta (D and E). White arrows indicate *scrib*-knockdown clones showing tumorigenic phenotype. Nuclei were labeled with DAPI (blue). Scale bar = 50 µm. The tumor phenotype of each clone was classified according to the flowchart shown in **Figure 1**. Detailed genotypes: **A-E,** *hsFLP; UAS-scrib-RNAi; act>CD2>GAL4, UAS-EGFP* (heat-shocked 30 min at 2 days AED, incubate 4 days at 25 ˚C after heat shock). Please click here to view a larger version of this figure.

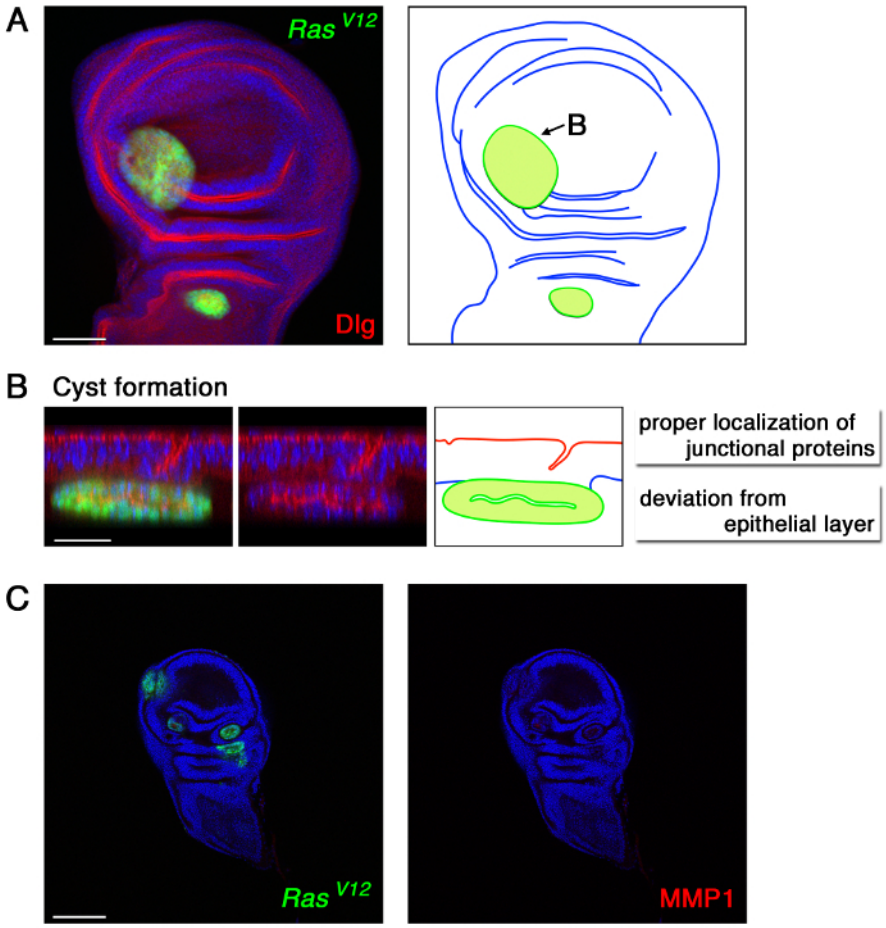

Figure 6: Diagnostic Examination of *Ras*^{V12}-expressing Clonal Phenotypes. (**A**) The left panel shows a mosaic wing imaginal disc of third instar larva with clones co-expressing oncogenic *Ras*^{V12} and GFP (green) 4 days after heat-shock induction, stained for Dlg (red). The right panel shows a schematic line drawing of the apical side of the epithelial layers (blue) and the GFP-expressing clones (green). Scale bar represents 50 µm. (**B**) Vertical sections of the *Ras*^{V12} expressing clones indicated in the right panel of (A). The second panels from the left show the Dlg localization patterns (red). The third panels from the left show schematic line drawings of the apical (red) and basal (blue) sides of epithelial layers and the *Ras*^{V12} and GFP expressing clones (green). Scale bar = 25 µm. (**C**) Mosaic wing imaginal disc of third instar larva with clones co-expressing *Ras*^{V12} and GFP (green) 4 days after heat-shock induction, stained for MMP1 (red). Scale bar = 100 µm. Detailed genotypes: **A-C,** *hsFLP; UAS-Ras*^{V12}*; act>CD2>GAL4, UAS-EGFP* (heat-shocked 45 min at 2 days AED, incubate 4 days at 25 °C after heat shock). Please click here to view a larger version of this figure.

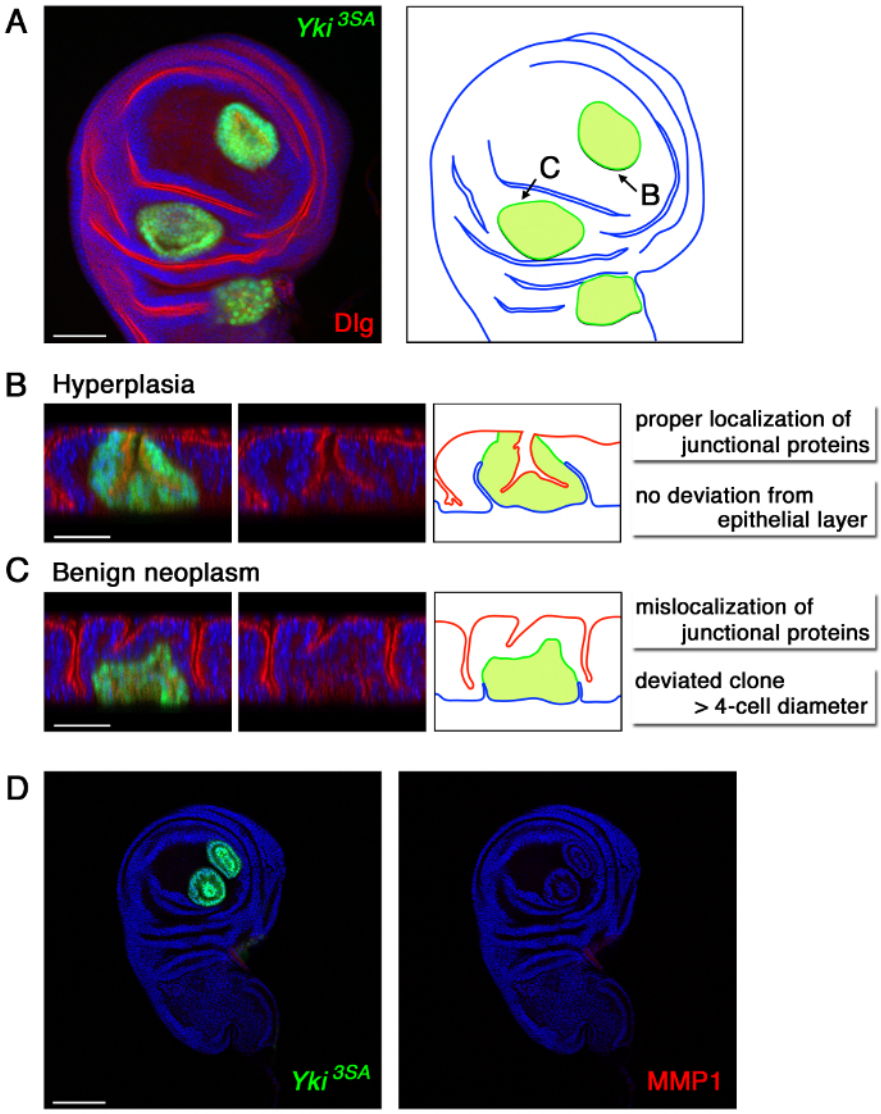

Figure 7: Diagnostic Examination of *Yki*^{3SA}-expressing Clonal Phenotypes. (**A**) The left panel shows a mosaic wing imaginal disc of third instar larva with clones co-expressing constitutively active *Yki*^{3SA} and GFP (green) 4 days after heat-shock induction, stained for Dlg (red). The right panel shows a schematic line drawing of the apical side of the epithelial layers (blue) and the GFP-expressing clones (green). Scale bar = 50 µm. (**B-C**) Vertical sections of the *Yki*^{3SA} expressing clones indicated in the right panel of (A). The second panels from the left show the Dlg localization patterns (red). The third panels from the left show schematic line drawings of the apical (red) and basal (blue) sides of epithelial layers and the *Yki* and GFP expressing clones (green). Scale bar = 25 µm. (**D**) Mosaic wing imaginal disc of third instar larva with clones co-expressing *Yki*^{3SA} and GFP (green) 4 days after heat-shock induction, stained for MMP1 (red). Scale bar = 100 µm. Detailed genotypes: **A-D,** *hsFLP;; UAS-Yki*^{3SA}*/ act>CD2>GAL4, UAS-EGFP* (heat-shocked 30 min at 2 days AED, incubate 4 days at 25 °C). Please click here to view a larger version of this figure.

Discussion

The GAL4-UAS system is one of the most powerful genetic tools for targeted gene expression in *Drosophila* [26] and greatly facilitates tumor cell induction and analysis *in vivo* [4]. This system enables the generation of clones bearing knockdown of tumor-suppressor genes or overexpression of oncogenes within wild-type epithelial tissue, a situation highly similar to the initial stages of human cancer where transformed pro-tumor cells are surrounded by normal epithelial cells. GAL4 driver lines regulated by enhancer sequences such as GAL4 enhancer-trap lines or Janelia GAL4 lines [27] have unique, spatiotemporally restricted expression patters. Therefore, these enhancer-GAL4 lines are useful to induce tumors consistently in restricted areas of imaginal discs. In addition to *sd-GAL4* and *upd-GAL4* shown in this study, we confirmed that *lgl*-knockdown induced by other enhancer-trap GAL4 lines including *engrailed-GAL4* (*en-GAL4*), *hedgehog-GAL4* (*hh-GAL4*), *optomotor-blind-GAL4* (*omb-GAL4*), *patched-GAL4* (*ptc-GAL4*) and *spalt-major-GAL4* (*salm-GAL4*) can generate neoplastic tumors in the hinge regions of wing imaginal discs. If the enhancer-GAL4 expression pattern needs to be temporally controlled, a combination of GAL4 and a temperature-sensitive version of GAL80 (GAL80^{ts}) is an option. GAL80^{ts} represses GAL4 function at 18 °C but not at 29 °C, which permits UAS-transgenes expression to be switched on or off as necessary [28].

The flip-out-GAL4 mosaic system, which combines the FLP-FRT system and the GAL4-UAS system [3], generates random clones in imaginal discs. By combining heat-shock-inducible flippase (hsFLP) with flip-out GAL4, the timing of clone generation is controllable. Because the tumorigenic potential of imaginal disc cells may be dependent on the developmental stage, endogenous signaling events, and/or cellular differentiation [29,30], it is very important to examine the effect of altered heat-shock timing on tumorigenic phenotypes.

It has been previously shown that nTSG mutant clones undergo cell competition-dependent apoptosis when surrounded by wild-type cells [10,11,12,18], suggesting that multiple mutations are required for cell transformation during cancer development. In fact, overexpression of oncogenic Ras or Yki in *lgl* or *scrib* mutant clones transforms them into aggressive tumors [10,18,31] whereas misexpression of Ras^{V12} or Yki^{3SA} does not induce malignant neoplasm by themselves without nTSG mutations. As shown here and previously [16], pro-tumor nTSG-knockdown clones generated in wild-type wing discs also undergo apoptosis and do not show tumorigenesis in the wing pouch [16]. At the same time, nTSG-knockdown clones located in hinge "hotspots" develop into neoplastic tumors without any additional oncogenic mutations. In hinge regions, nTSG-deficient cells hijack endogenous Janus kinase/signal transducer and activator of transcription (JAK/STAT) signaling to drive tumorigenesis [16]. Therefore, hinge-specific GAL4s such as *upd-GAL4* are useful tools for consistently inducing neoplastic tumor formation by *RNAi*-mediated knockdown of tumor suppresser genes. Although flip-out-GAL4-induced nTSG-knockdown mosaic clones also induce neoplastic tumors in hinge regions, tumorigenesis occurrence is dependent on initial clone size: large clones generated by a heat shock over 20 min usually induce tumorigenesis, whereas most small clones generated by heat shock shorter than 10 min are completely eliminated (K.M. and Y.T., unpublished data).

A number of recent studies on tumor development and cancer progression use *Drosophila* imaginal discs as a model system [32,33]. Common to these studies include several markers of neoplastic tumors: deviant cell masses, deformed disc shapes, accumulation of F-actin, enhanced cell cycling (BrdU/EdU incorporation or PH3 expression), activation of JNK signaling and its downstream target MMP1, basement membrane disruption, and/or epithelial disorganization, including loss or subcellular delocalization of proteins involved in apical-basal cell polarity (Crumbs, Stardust, PatJ, aPKC, Bazooka/PAR-3 or PAR-6), septate junctions (Lgl, Scrib, Dlg or Coracle), or adherens junctions (E-Cadherin or Armadillo). These phenotypes are readily detectable by conventional antibody staining. Although it is difficult to determine if a clonal phenotype is hyperplasia, dysplasia, benign neoplasm or malignant neoplasm in the early stage of tumorigenesis, it should be simpler in the *Drosophila* imaginal disc epithelia composed of a single epithelial monolayer. In this study, we introduced a diagnosis method to classify tumorous clone phenotypes induced in the epithelial monolayer (**Figure 1**). This method requires careful observations of five criteria using z-stack confocal images; each diagnostic criterion can be examined by conventional antibody staining and confocal imaging. One of the new criteria we introduced in this method is "4-cell-diameter criteria" which discriminates between dysplasia and neoplasm in imaginal discs. Pro-tumor cells such as nTSG mutant clones are frequently extruded from epithelial layers through cell competition or spindle misorientation [15,16,34]. In most situations, these extruded cells apoptose, and so they cannot proliferate. Although it might be possible that the pro-tumor cells undergo cell division once during extrusion and once or twice more after extrusion, this makes a cell mass of 2- to 3-cell diameter. Therefore, if a cell mass of pro-tumor cells deviated from epithelial layer is larger than 4-cell diameter, we can determine that they are surviving and proliferating as a neoplasm outside of the epithelial layer.

Although this diagnosis method is simple, it is critical to take a time course of phenotypes, as tumor development and malignancy progresses throughout time. For example, dysplasia is a cytologically abnormal tissue and a transitional state between completely benign growths and those that are premalignant. Therefore, even if an observed clone is defined as a dysplasia according to the flowchart (**Figure 1**), it is possible that the dysplasia subsequently develops into a neoplasm. Although the larval stage is limited in time (5 - 6 days at 25 °C or 4 - 5 days at 29 °C AED), tumor growth in imaginal discs prolongs the larval stage through an insulin-like peptide induced delay of pupariation [35,36]. Therefore, neoplastic tumor formation in imaginal discs makes it possible to observe tumor clone phenotypic progression for several more days. Our simple classification method might be broadly applicable to the clonal analysis of tumor phenotypes in various organs in *Drosophila*.

Disclosures

The authors have nothing to disclose.

Acknowledgements

We thank J. Vaughen for critical reading of the manuscript. This work was supported by grants from JSPS KAKENHI Grant Numbers 26891025, 15H01500 and The Takeda Science Foundation Research Grant to Y.T.

References

1. Hanahan, D., & Weinberg, R. A. The hallmarks of cancer. *Cell.* **100** (1), 57-70 (2000).
2. Xu, T., & Rubin, G. M. Analysis of genetic mosaics in developing and adult Drosophila tissues. *Development.* **117** (4), 1223-1237 (1993).
3. Struhl, G., & Basler, K. Organizing activity of wingless protein in Drosophila. *Cell.* **72** (4), 527-540 (1993).
4. Potter, C. J., Turenchalk, G. S., & Xu, T. Drosophila in cancer research. An expanding role. *Trends Genet.* **16** (1), 33-39 (2000).
5. Miles, W. O., Dyson, N. J., & Walker, J. A. Modeling tumor invasion and metastasis in Drosophila. *Dis Model Mech.* **4** (6), 753-761 (2011).
6. Tipping, M., & Perrimon, N. Drosophila as a model for context-dependent tumorigenesis. *J Cell Physiol.* **229** (1), 27-33 (2013).
7. Bilder, D. Epithelial polarity and proliferation control: links from the Drosophila neoplastic tumor suppressors. *Genes Dev.* **18** (16), 1909-1925 (2004).
8. Humbert, P. O., *et al.* Control of tumourigenesis by the Scribble/Dlg/Lgl polarity module. *Oncogene.* **27** (55), 6888-6907 (2008).
9. Huang, L., & Muthuswamy, S. K. Polarity protein alterations in carcinoma: a focus on emerging roles for polarity regulators. *Curr Opin Genet Dev.* **20** (1), 41-50 (2010).
10. Brumby, A. M., & Richardson, H. E. scribble mutants cooperate with oncogenic Ras or Notch to cause neoplastic overgrowth in Drosophila. *EMBO J.* **22** (21), 5769-5779 (2003).

Copyright © 2017 Journal of Visualized Experiments

11. Igaki, T., Pastor-Pareja, J. C., Aonuma, H., Miura, M., & Xu, T. Intrinsic tumor suppression and epithelial maintenance by endocytic activation of Eiger/TNF signaling in Drosophila. *Dev Cell.* **16** (3), 458-465 (2009).
12. Tamori, Y., *et al.* Involvement of Lgl and Mahjong/VprBP in cell competition. *PLoS Biol.* **8** (7), e1000422 (2010).
13. Cordero, J. B., *et al.* Oncogenic Ras diverts a host TNF tumor suppressor activity into tumor promoter. *Dev Cell.* **18** (6), 999-1011 (2010).
14. Yamamoto, M., Ohsawa, S., Kunimasa, K., & Igaki, T. The ligand Sas and its receptor PTP10D drive tumour-suppressive cell competition. *Nature.* 542(7640), 246-250 (2017).
15. Vaughen, J., & Igaki, T. Slit-Robo Repulsive Signaling Extrudes Tumorigenic Cells from Epithelia. *Dev Cell.* **39** (6), 683-695 (2016).
16. Tamori, Y., Suzuki, E., & Deng, W.-M. Epithelial Tumors Originate in Tumor Hotspots, a Tissue-Intrinsic Microenvironment. *PLoS Biol.* **14** (9), e1002537-23 (2016).
17. Ohsawa, S., *et al.* Elimination of oncogenic neighbors by JNK-mediated engulfment in Drosophila. *Dev Cell.* **20** (3), 315-328 (2011).
18. Menéndez, J., Pérez-Garijo, A., Calleja, M., & Morata, G. A tumor-suppressing mechanism in Drosophila involving cell competition and the Hippo pathway. *Proc Natl Acad Sci U S A.* **107** (33), 14651-14656 (2010).
19. Hogan, C., *et al.* Characterization of the interface between normal and transformed epithelial cells. *Nat Cell Biol.* **11** (4), 460-467 (2009).
20. Kajita, M., *et al.* Interaction with surrounding normal epithelial cells influences signalling pathways and behaviour of Src-transformed cells. *J Cell Sci.* **123** (Pt 2), 171-180 (2010).
21. Norman, M., *et al.* Loss of Scribble causes cell competition in mammalian cells. *J Cell Sci.* **125** (1), 59-66 (2012).
22. Wagstaff, L., *et al.* Mechanical cell competition kills cells via induction of lethal p53 levels. *Nat Commun.* **7**, 1-14 (2016).
23. Kajita, M., & Fujita, Y. EDAC: Epithelial defence against cancer-cell competition between normal and transformed epithelial cells in mammals. *J Biochem.* **158** (1), 15-23 (2015).
24. North, A. J. Seeing is believing? A beginners' guide to practical pitfalls in image acquisition. *J Cell Biol.* **172** (1), 9-18 (2006).
25. Schindelin, J., *et al.* Fiji: an open-source platform for biological-image analysis. *Nat Methods.* **9** (7), 676-682 (2012).
26. Brand, A. H., & Perrimon, N. Targeted gene expression as a means of altering cell fates and generating dominant phenotypes. *Development.* **118** (2), 401-415 (1993).
27. Jory, A., *et al.* A survey of 6,300 genomic fragments for cis-regulatory activity in the imaginal discs of Drosophila melanogaster. *Cell Rep.* **2** (4), 1014-1024 (2012).
28. McGuire, S. E., Le, P. T., Osborn, A. J., Matsumoto, K., & Davis, R. L. Spatiotemporal rescue of memory dysfunction in Drosophila. *Science.* **302** (5651), 1765-1768 (2003).
29. Rodrigues, A. B., *et al.* Activated STAT regulates growth and induces competitive interactions independently of Myc, Yorkie, Wingless and ribosome biogenesis. *Development.* **139** (21), 4051-4061 (2012).
30. Khan, S. J., *et al.* Epithelial neoplasia in Drosophila entails switch to primitive cell states. *Proc Natl Acad Sci U S A.* **110** (24), E2163-72 (2013).
31. Pagliarini, R. A., & Xu, T. A genetic screen in Drosophila for metastatic behavior. *Science.* **302** (5648), 1227-1231 (2003).
32. Gonzalez, C. Drosophila melanogaster: a model and a tool to investigate malignancy and identify new therapeutics. *Nat Rev Cancer.* **13** (3), 172-183 (2013).
33. Patel, P. H., & Edgar, B. A. Tissue design: how Drosophila tumors remodel their neighborhood. *Semin Cell Dev Biol.* **28**, 86-95 (2014).
34. Nakajima, Y.-I., Meyer, E. J., Kroesen, A., McKinney, S. A., & Gibson, M. C. Epithelial junctions maintain tissue architecture by directing planar spindle orientation. *Nature.* **500** (7462), 359-362 (2013).
35. Colombani, J., Andersen, D. S., & Léopold, P. Secreted peptide Dilp8 coordinates Drosophila tissue growth with developmental timing. *Science.* **336** (6081), 582-585 (2012).
36. Garelli, A., Gontijo, A. M., Miguela, V., Caparros, E., & Dominguez, M. Imaginal discs secrete insulin-like peptide 8 to mediate plasticity of growth and maturation. *Science.* **336** (6081), 579-582 (2012).

Copyright © 2017 Journal of Visualized Experiments